View metadata, citation and similar papers at core.ac.uk

brought to you by CORE

provided by UNT Digital Library

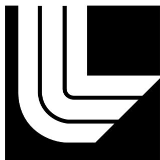

LAWRENCE
LIVERMORE
NATIONAL
LABORATORY

UCRL-CONF-229030

Critical parameters influencing the EUV-induced damage of Ru-capped multilayer mirrors

S. B. Hill, I. Ermanoski, C. Tarrio, T. B. Lucatorto, T. E. Madey, S. Bajt, M. Fang, M. Chandhok

March 13, 2007

SPIE Advanced Lithography
San Jose, CA, United States
February 25, 2007 through March 2, 2007

Disclaimer

This document was prepared as an account of work sponsored by an agency of the United States Government. Neither the United States Government nor the University of California nor any of their employees, makes any warranty, express or implied, or assumes any legal liability or responsibility for the accuracy, completeness, or usefulness of any information, apparatus, product, or process disclosed, or represents that its use would not infringe privately owned rights. Reference herein to any specific commercial product, process, or service by trade name, trademark, manufacturer, or otherwise, does not necessarily constitute or imply its endorsement, recommendation, or favoring by the United States Government or the University of California. The views and opinions of authors expressed herein do not necessarily state or reflect those of the United States Government or the University of California, and shall not be used for advertising or product endorsement purposes.

Critical parameters influencing the EUV-induced damage of Ru-capped multilayer mirrors

S. B. Hill[a], I. Ermanoski[a], C. Tarrio[a], T. B. Lucatorto[a], T. E. Madey[b], S. Bajt[†c], M. Fang[d], M. Chandhok[d]

[a]NIST, 100 Bureau Drive, Stop 8411, Gaithersburg, MD 20853-8411
[b]Rutgers University, 136 Frelinghuysen Rd.,Piscataway, NJ 08854-8019
[c]Lawrence Livermore National Laboratory, 7000 East Avenue, Livermore, CA 94550
[d]Intel Corporation, 2111 NE 25th Ave., Hillsboro, OR 97124

ABSTRACT

Ongoing endurance testing of Ru-capped multilayer mirrors (MLMs) at the NIST synchrotron facility has revealed that the damage resulting from EUV irradiation does not always depend on the exposure conditions in an intuitive way. Previous exposures of Ru-capped MLMs to EUV radiation in the presence of water vapor demonstrated that the mirror damage rate actually decreases with increasing water pressure. We will present results of recent exposures showing that the reduction in damage for partial pressures of water up to $5x10^{-6}$ Torr is not the result of a spatially uniform decrease in damage across the Gaussian intensity distribution of the incident EUV beam. Instead we observe a drop in the damage rate in the center of the exposure spot where the intensity is greatest, while the reflectivity loss in the wings of the intensity distribution appears to be independent of water partial pressure. (See Fig. 1.) We will discuss how the overall damage rate and spatial profile can be influenced by admixtures of carbon-containing species (e.g., CO, CO_2, C_6H_6) at partial pressures one-to-two orders of magnitude lower than the water vapor partial pressure. An investigation is underway to find the cause of the non-Gaussian damage profile. Preliminary results and hypotheses will be discussed. In addition to high-resolution reflectometry of the EUV-exposure sites, the results of surface analysis such as XPS will be presented. We will also discuss how the bandwidth and time structure of incident EUV radiation may affect the rate of reflectivity degradation. Although the observations presented here are based on exposures of Ru-capped MLMs, unless novel capping layers are similarly characterized, direct application of accelerated testing results could significantly overestimate mirror lifetime in the production environment.

Keywords: extreme ultraviolet; lithography; reflectometry; EUV optics; ruthenium films; lifetime testing

1. INTRODUCTION

Commercialization of extreme-ultraviolet lithography (EUVL) presents a number of significant technical challenges, including pushing metrology to new limits. The Photon Physics Group of the National Institute of Standards and Technology (NIST) has been involved in developing and providing EUVL metrology for almost two decades. In fact, the most mature program, EUV detector calibration,[1] has been operating at the Synchrotron Ultraviolet Radiation Facility (SURF III) storage ring since well before the birth of the EUVL effort. In 1988 we began a program for the measurement of reflectivities of EUV multilayer (ML) optics.[2] Most recently we have constructed a beamline dedicated to long-term studies of ML lifetimes in a controlled environment.[3]

The requisite MLM lifetime is 30,000 hours, or about 3.5 years of continuous operation without a decrease in reflectivity of more than a few percent. With a predicted EUVL insertion point around 2010, developers cannot test

[†] This work was performed under the auspices of the U.S. Department of Energy by University of California Lawrence Livermore National Laboratory under contract No. W-7405-Eng-48

MLs for that period of time, necessitating the investigation of accelerated testing methods. In this paper, we will describe our program and offer results from selected lifetime-testing experiments.

2. MULTILAYER ENDURANCE TESTING

2.1. The optics lifetime problem for EUV lithography

EUV lithography employs a set of reflective optics to project the mask image onto the resist-covered wafer. The EUV mirrors are coated with an extremely precise ML coating consisting of 40 or more MoSi bilayers deposited with a ~ 7-nm period. Reflectivity approaching 70% is achieved through the constructive interference of the light rays with wavelength near 13.5 nm that are reflected from each of the appropriately spaced bilayers

The EUV mirrors are housed in a vacuum chamber called the projection optics (PO) box. Because baking the PO box would damage the mirrors by accelerating inter-diffusion of the MoSi bilayers and would destroy the precise alignment of the mirrors, the ambient background will contain residual water and hydrocarbon vapors. These trace gases can adsorb onto the optic surface and be fragmented by the energetic (91.8 eV) EUV photons or secondary electrons, producing reactive species. Oxygen atoms from dissociated water molecules can oxidize the mirror surface, while carbon from cracked hydrocarbon molecules can form a graphitic overlayer. An intensive effort is underway to develop a capping layer to protect the mirror surface from oxidation and carbon buildup because both cause undesirable reflectivity loss. The work presented here was performed using the first promising capping layer of Ru developed and fabricated at Lawrence Livermore National Labs.[4] NIST's contribution to the effort is the provision of long-term EUV exposure testing under vacuum conditions with controlled amounts of water vapor and carbonaceous contaminants.

2.2. EUV exposure facilities at NIST

A schematic of the original endurance testing facility on SURF III is shown in Fig. 1. The output of the synchrotron is collected by a near-normal-incident ML mirror placed approximately 4 m from the storage ring tangent point. This MLM is designed to reflect EUV radiation with a 10-degree angle of incidence in the bandwidth 13.1 nm to 13.6 nm with approximately 50% efficiency. The resulting focal spot is ~1.5 m downstream and has a Gaussian intensity distribution with a time-averaged peak of 7.7±1.0 mW/mm^2 and a full-width half-max of ~650 μm. A 200 nm-thick beryllium filter completely blocks long-wavelength light while transmitting 50-60% of the EUV radiation. More importantly, this filter also serves as a physical barrier separating the exposure chamber from the rest of the beamline. It is essential that the synchrotron and the focusing mirror not be exposed to the high levels of water and hydrocarbon vapors present in the exposure chamber during most endurance tests.

Since thermal diffusion of the ML structure would ruin the mirror to be tested, the exposure chamber can not be baked once the sample is installed. Instead the exposure chamber was constructed to meet UHV specifications and was pre-baked up to 150º C. To minimize contamination, the chamber is slightly over-pressured with dry N_2 to maintain a flow while new samples are loaded. In order to accelerate sample aging during testing, the partial pressure of water vapor in the exposure chamber can be varied between the base pressure of $<1\times10^{-9}$ Torr and 5×10^{-6} Torr, which is considerably greater than the expected base pressure in a stepper. Similar pressures of hydrocarbons can also be independently or simultaneously introduced. The average intensity at the test sample is at least 10 times the maximum intensity predicted on most optics in a commercial stepper.[4] This allows limited scaling studies to investigate the dependence of damage rate on various adjustable quantities that could be used to accelerate the lifetime tests.

A second end station with a similar optical layout was added to SURF for lifetime testing. In this chamber samples are exposed to an asymmetric Gaussian intensity distribution with a peak of 7.5±1.0 mW/mm^2 and full width-at-half maxima of 1092 μm and 534 μm. This new facility was designed to maximize throughput and minimize contamination associated with sample introduction. The chamber has a smooth electropolished finish, and most of the components exposed to vacuum are plated with a 0.5μm layer of gold to minimize adsorption of water and desorption of contaminant species from the chamber walls. The exposure chamber is bakeable to 150ºC, limited only by the photodiodes used to measure the intensity of the incident and reflected EUV radiation. Samples are introduced through a gold-plated loadlock. So, unlike the original system, the exposure chamber is not exposed to air each time a new

sample is tested. All pumps in both the new and original systems are completely oil free. The base pressure in the new chamber is routinely in the mid 10^{-11} Torr range.

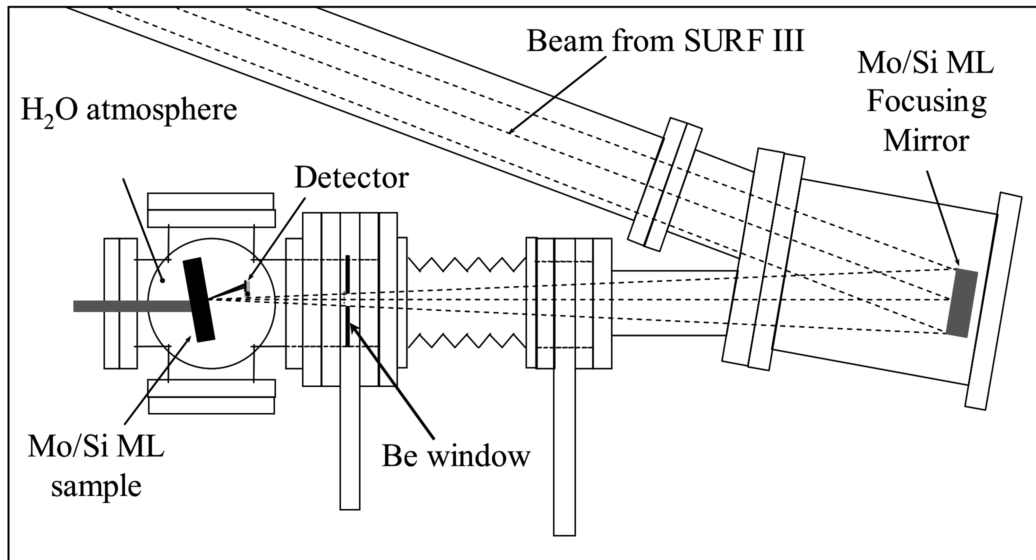

Fig. 1. Schematic of the original end-station on the SURF III synchrotron for endurance testing of EUV optics at NIST

In both chambers the MLM under test is placed at the focal spot of the EUV beam and oriented to reflect the incident radiation at 10 degrees. The reflectivity in the original chamber is monitored during exposures by a single Zr-coated silicon photodiode that can be rotated to measure the incident and reflected power. In the new chamber two Mo-Si coated photodiodes are used. These *in situ* measurements, however, lack the precision to accurately measure the critical 1-2% changes in reflectivity at 13.5 nm and do not provide any information on the spatial distribution of the damage. High spatial-resolution post-exposure reflectometry is performed at the Lawrence Berkeley Lab Advanced Light Source to accurately measure the reflectivity at 13.5 nm in 100-micrometer steps over the entire exposure spot. (Although the 0.3% absolute uncertainty of the reflectometer at NIST is certainly sufficient for this task, the Berkeley facility provides slightly better spatial resolution.)

3. RESULTS OF ENDURANCE TESTING AT NIST SYNCHROTRON

Over the past three years we have exposed MLMs with capping layers of Si, Ru and TiOx for both our own studies as well as for industrial customers. The results presented here reflect only the independent studies carried out by the NIST and Rutgers co-authors on Ru-capped MLMs prepared by Sasa Bajt at the Lawrence Livermore National Laboratory.[4] As discussed below, we investigated the dependence of mirror damage on both the intensity and bandwidth of the incident EUV radiation as well as on the partial pressure of admitted water vapor.

3.1. Effect of admitted water vapor

Initial 10-hour (190 J/mm^2) EUV exposures of Ru-capped MLMs in the presence of admitted water vapor produced the surprising result of decreasing mirror damage with increasing water-vapor partial pressure.[5] Figure 2 shows the reflectivity losses at the center of the exposure spot of several 10-hour exposures under varying conditions of ambient water vapor pressure and average EUV intensity. Both the high and low intensity exposures display the non-intuitive inverse relationship between reflectivity loss and water-vapor partial pressure; however, this effect is more prominent in the lower intensity exposures with dose ~95 J/mm^2.

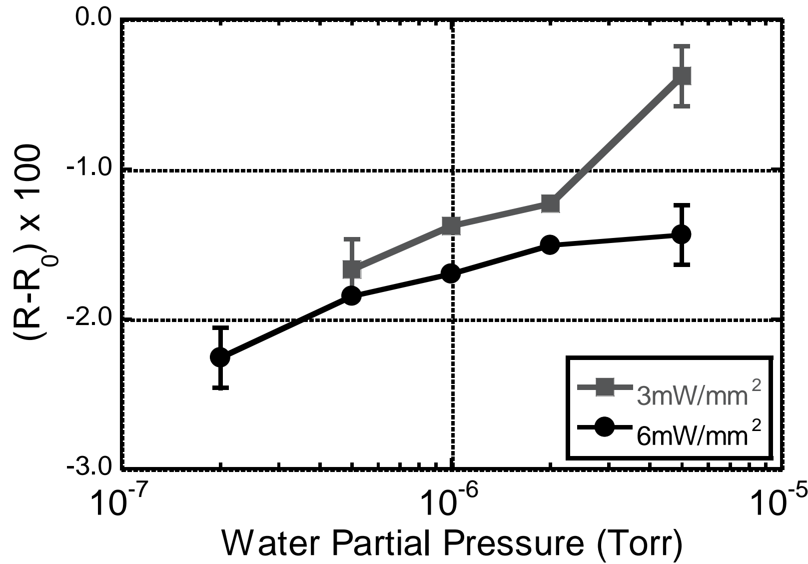

Fig. 2. Change in reflectivity at the center of the exposure spots as a function of water partial pressure at two different average EUV intensities. Error bars represent combined uncertainty of absolute reflectivity measurements of exposed and unexposed (R_0) areas.

In order to monitor the water pressure in the exposure chamber, these initial exposures were performed with a Bayard-Alpert-type ion gauge and a quadrupole mass spectrometer residual gas analyzer (RGA) turned on. The hot filament of the RGA was well shielded and behind the sample, but the ion gauge was approximately 10 cm away and oriented nearly parallel to the surface of the sample. To investigate whether the hot filaments were playing a role in the non-intuitive behavior demonstrated in Fig. 2, the exposures were repeated with all filaments turned off. The results of peak reflectivity loss as a function of water pressure were similar to those with the filaments on. High-spatial-resolution reflectometry of the exposure spot, however, revealed that the spatial distribution of the damage departed significantly from the measured Gaussian profile of the incident EUV beam.

Figures 3(a) and 3(b) show the reflectivity measured along a line through the center of several exposure spots normalized to the native reflectivity of the unexposed MLM. The results are for ~10 hr exposures with different partial pressures of water vapor and an average dose of 170 J/mm^2 or 190 J/mm^2. The exposures in (a) took place in the absence of any hot filaments, but the ion gauge and RGA were both on during the exposures plotted in (b). The measured intensity distribution of the incident EUV beam is also shown for comparison.

The inverse water-vapor-pressure dependence of reflectivity loss for exposures with filaments off in Fig. 3(a) is more pronounced near the center of the beam where the intensity and hence dose are highest. In fact, the 5x10^{-6} Torr exposure with the slightly higher average dose shows almost no decrease in reflectivity in the center, while the losses in the low-intensity wings are nearly independent of water pressure. The reflectivity profiles in Fig. 3(b), however, show exactly the opposite behavior when the filaments are left on during the exposure. In this case, the reflectivity loss near the high-dose beam center is still smaller for the larger pressure, but this difference is significantly less than that for lower doses in the wings of the EUV distribution. The evolution with dose of these highly non-linear damage profiles is discussed in Sec. 3.3 below.

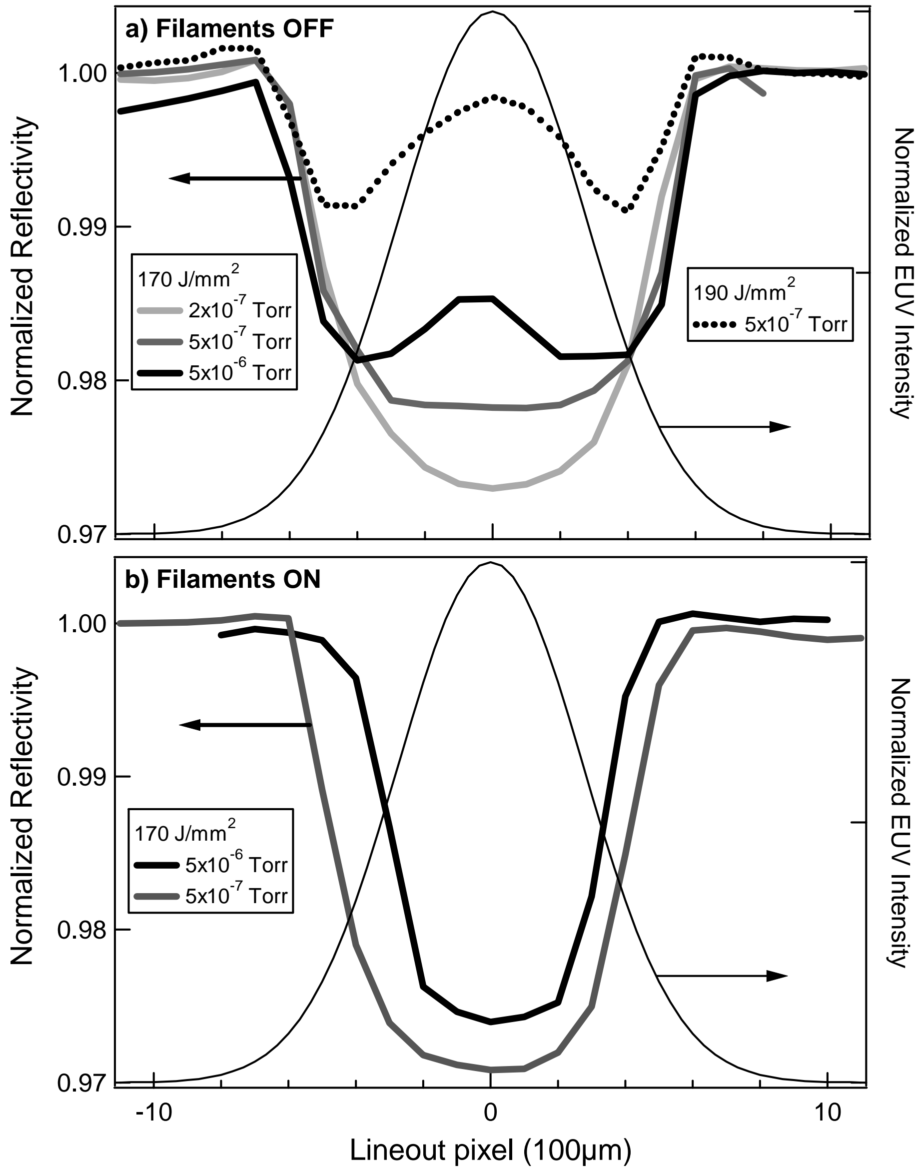

Fig. 3. The measured spatial distribution of reflectivity for several exposure spots is plotted along a line through the center of each spot. The H_2O partial pressure and average dose are indicated. The measured Gaussian distribution of EUV intensity (7.7 mW/mm^2 at the peak) is also shown. (a) When there are no ion gauge or other hot filaments present the decrease in damage with increasing H_2O partial pressure is most pronounced at the highest doses near the center of the beam, while there is little variation with pressure for the lower doses in the wings. There is almost no reflectivity loss at the center of the slightly higher dose exposure in $5x10^{-6}$ Torr H_2O. (b) Having the filaments on during the exposure still produced the inverse dependence of damage with H_2O pressure, but this effect is smallest at the highest doses near the center and greatest in the low-dose wings.

3.2. Effects of simple carbon-containing gases

One possible reason for this unexpected result is that there is a mixture of water and hydrocarbon vapors in the exposure chamber. As demonstrated by Klebanoff,[6] the damage caused by EUV+H_2O can be significantly mitigated by admitting a mixture of ethanol and water at comparable partial pressures. It is thought that the C species produced by EUV cracking of the ethanol react with the potentially oxidizing O and OH radicals to form CO and/or CO_2 which then leaves the surface. In this way the two potentially damaging reactions of carbon deposition and oxidation actually compete with each other producing much less damage to the mirror surface than either process alone. We confirmed this by exposing samples to EUV in the presence of an admixture of water and methanol vapors. Surprisingly the damage caused by 10-hr exposures in $1x10^{-6}$ Torr of water is completely mitigated by an admixture of just $2x10^{-8}$ Torr of methanol.[5]

While this test demonstrated that damage by oxidation can be dramatically affected by just a few parts per thousand of methanol, the only carbon-containing gases detected by RGA analysis of the exposure environment were CO and CO_2. To see whether these gases would have a similar effect, we performed independent 10-hour exposures in admixtures of water and either CO or CO_2 directly admitted at levels exceeding those present in the ambient vacuum. Unlike methanol, these simple carbonaceous species had no measurable effect on the EUV+H_2O damage rate of the MLMs whether the ion gauge and RGA filaments were on or not. So they would not likely play a role in the inverse dependence of damage on water vapor pressure demonstrated in Fig. 2.

We also performed similar tests with admixtures of water and H_2, which is the only other significant background gas. Admission of $5x10^{-7}$ Torr water vapor alone increased the H_2 RGA peak from a base level of $1x10^{-10}$ Torr to $2x10^{-9}$ Torr, but exposures in an admixture of $5x10^{-7}$ Torr water and to $1x10^{-8}$ Torr of directly admitted H_2 produced results identical to those with water alone. Surprisingly, if the partial pressures of water and H_2 were both $5x10^{-7}$ Torr, the reflectivity loss was ~30% greater than with water alone. Furthermore, when the same exposure was carried out with the ion gauge and RGA filaments activated, the damage was nearly 80% greater than the water-only loss. These observations appear to be at odds with the use of H_2 and atomic-H to clean carbon-deposits and oxidation from Ru-capped MLMs.[7] The conditions in these two cases, however are quite different. In the cleaning case, the H2 partial pressure is >10 mTorr, no water is admitted and no EUV radiation is incident on the surface. Nevertheless, the observed increase in damage resulting from EUV exposure in equal parts water and H_2 is not understood.

Although RGA analysis showed no evidence of large-mass (≤200 amu/e) hydrocarbons in our chamber, we used x-ray photoelectron spectroscopy (XPS) to directly look for signs of C deposition. Since the characteristic XPS peaks for Ru and C both occur at ~87 eV, it is very difficult to detect small amounts of C on top of Ru-capped MLMs. The 2p Si XPS peak, on the other hand, is near 103 eV. So it is quite easy to measure the carbon coverage as the ratio of the 1s C and 2p Si XPS peaks on Si-capped MLMs. This quantity is plotted in Fig. 4 for two different Si-capped MLM samples both exposed to 700 J/mm^2 under UHV conditions and to 700 J/mm^2 and 300 J/mm^2 in the presence of $2x10^{-7}$ Torr of water vapor. Sample B was cleaned with acetone and methanol and blown dry with nitrogen before exposure. Sample A was exposed after only a dusting with nitrogen, which is the standard practice. The native C content of sample A is ~30% higher than that for sample B indicating that a significant amount of surface contamination was removed by the pre-exposure solvent cleaning. Despite this difference in initial contamination, both samples experienced "EUV cleaning" that reduced the C content to ~60% of their native values when exposed in the UHV environment. The lower dose in water also reduced the C coverage for both samples but to a lesser extent. Exposure to the full 700 J/mm^2 in the presence of $2x10^{-7}$ Torr H_2O actually increased the carbon content of sample B above the native value, while the carbon concentration on the initially dirtier sample A was reduced. This suggests that there could be two forms of carbon affecting the degradation of reflectivity. The carbon species initially present on the unexposed surface could be reduced by both solvent cleaning and EUV exposure, while exposure to EUV would deposit a second, less volatile species. Whatever the case, the increase in C coverage with exposure time implies that the primary source of EUV-induced C deposition in water vapor is from ambient carbon-containing gases rather than from EUV cracking of native surface contaminants. The time evolution of the damage, however, would likely be influenced by the degree of EUV-cleaning necessary to remove any initial surface contamination.

These findings suggest that EUV exposures in the presence of water vapor can cause both oxidation and C deposition on Si-capped MLMs. While the reaction kinetics for EUV-induced C deposition may be different for Ru and Si, EUV-induced C growth is possible even though there is no evidence of hydrocarbons in the RGA spectrum. The C could come from impurities in the water, but only HPLC semiconductor-grade water was used with well-baked tubing and valves. Furthermore RGA analysis revealed no impurities above the 10^{-10} Torr level even at 10^{-5} Torr partial pressures of H_2O. It is possible that C growth on the surface is actually due to a radical or even ionic carbon species created by EUV light incident on the chamber walls. Such a reactive species would emanate from the illuminated portions of the chamber and likely react with the first surface encountered; therefore, it would not exist as an equilibrium vapor detectable by the RGA. We intend to test this hypothesis by placing Si witness plates facing towards and away from the EUV-illuminated wall but out of the direct beam. While this conjecture of radical species is purely hypothetical, the interaction of admitted gasses with otherwise non-volatile compounds on UHV chamber walls is a well known and carefully avoided phenomenon in surface physics.[8]

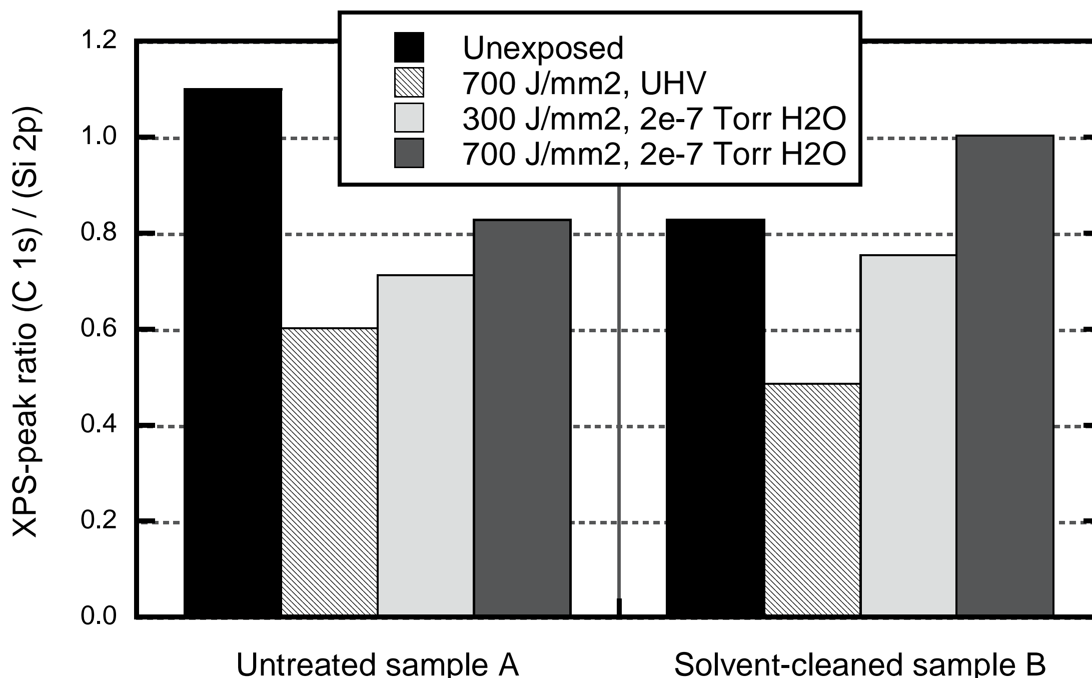

Fig. 4. Ratio of carbon 1s and Si 2p XPS peaks from Si-capped multilayer mirrors exposed to EUV under different conditions. Sample A was only dusted with nitrogen prior to exposure. Sample B was cleaned with acetone and methanol then blown dry with nitrogen. Solvent cleaning appears to have lowered native carbon content of surface. Both show a decrease in carbon content when exposed to an EUV dose of 700 J/mm^2 in UHV environment, but the C coverage of the solvent-cleaned sample increases above the native value when exposed to the same dose in $2x10^{-7}$ Torr H_2O.

3.3. Dose and intensity dependence of damage

To further investigate the non-Gaussian damage profiles observed at high water pressures, a series of exposures of varying duration were performed at $5x10^{-6}$ Torr H_2O in the absence of filaments. The evolution of the damage is illustrated in Fig. 5(a) by plotting the line-out profiles of the spatial distribution of reflectivity for these exposures spaced in proportion to exposure time. Since the EUV intensity is known at each point in the spatial profiles, the reflectivity loss at a given intensity can be extracted for each exposure shown in Fig. 5(a). For example, the dashed line indicates the loss in reflectivity as a function of time for the peak intensity of 7.7 mW/mm^2. This peak-intensity data is plotted in Fig. 5(b) as a function of dose along with the corresponding data for intensities 80, 60, 40 and 20 per-cent of the peak value.

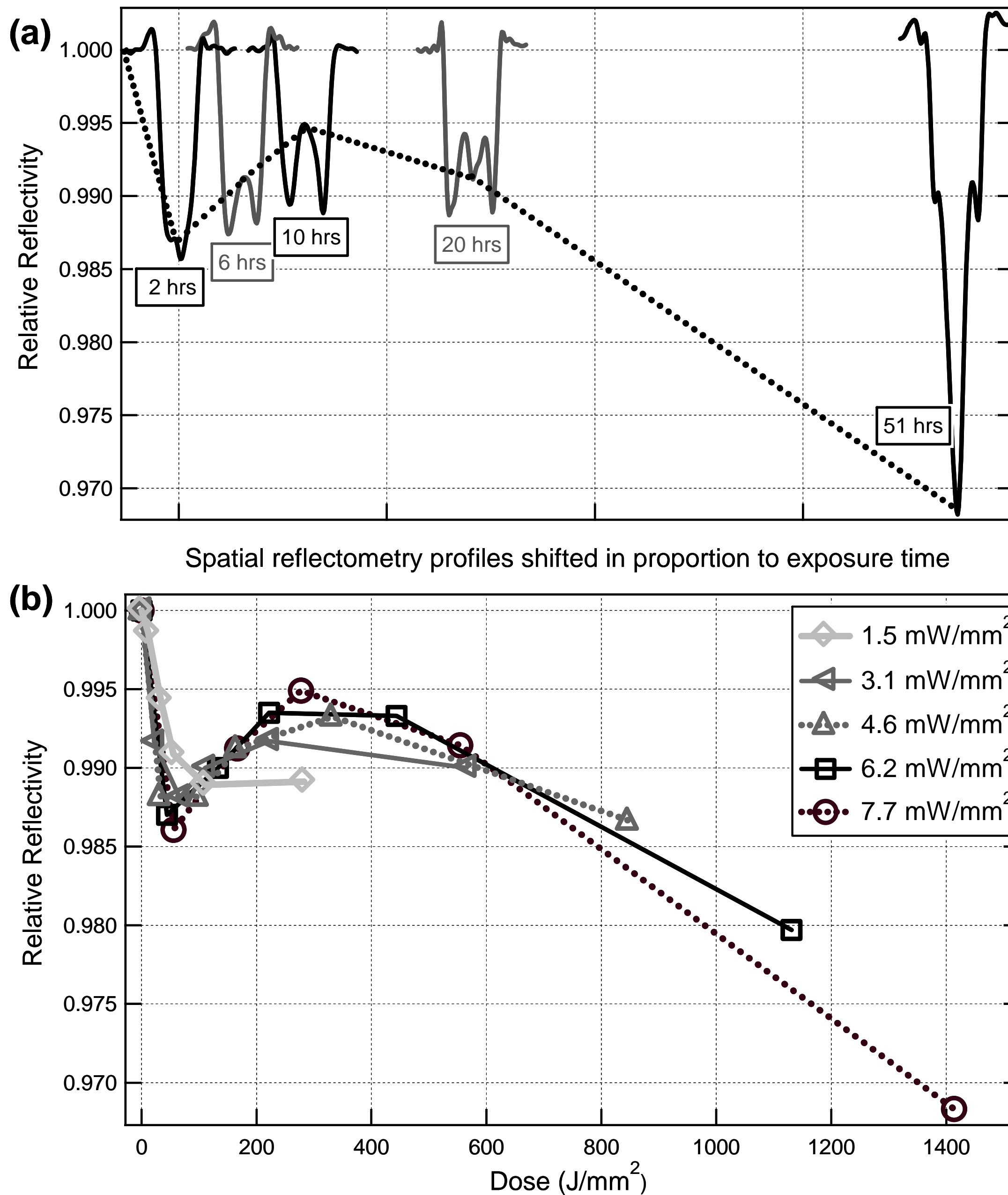

Fig. 5. (a) Spatial profiles of reflectivity following EUV exposure of different lengths in 5x10^{-6} Torr H_2O. Each profile is spaced horizontally in proportion to its duration. The dashed line connects the points of equal intensity at the center of the exposure beam for each exposure. (b) The reflectivity as a function of dose for different EUV intensities. The data for each intensity is calculated by correlating the known EUV intensity distribution with the damage profiles plotted in (a).

The plots in Fig. 5 clearly demonstrate a highly non-linear evolution of the reflectivity loss with dose. The same trend of initial damage followed by recovery and then an apparently linear reflectivity loss with dose is evident for all intensities in Fig. 5(b). The degree of nonlinearity, however, decreases with intensity. For example, the increase in

reflectivity starting around 50 J/mm^2 is quite pronounced for the highest intensity of 7.7 mW/mm^2. The increase is much less dramatic for 3.1 mW/mm^2, and for the lowest intensity case of 1.5 mW/mm^2 there does not appear to be a significant increase. Similarly, the rate of damage with dose in the approximately linear regime beyond 500 J/mm^2 appears larger for larger intensities. This suggests that there is not a simple relationship between damage and intensity even for doses much greater than those that produce the non-intuitive loss-recovery behavior, at least for the aggressive condition of 5x10^{-6} Torr H_2O vapor presented here. Similar studies at water-vapor pressures closer to tool conditions are planned.

This unexpected evolution of damage may be the result of competing oxidation and carbon-growth processes. The XPS data discussed in the previous section suggests that in addition to oxidation, EUV exposure may induce both growth and removal of carbon in different forms. Each of these reactions would likely depend differently on water-vapor pressure, EUV intensity and dose. Even if these were simple first-order reactions, the interaction of the reactants and products could result in they type of non-linear evolution displayed in Figures 5 (a) and (b).

3.4. Wavelength considerations

The constructive interference responsible for producing the high reflectivity of a MLM depends on a resonance between the carefully designed periodicity of the multilayer and the wavelength and angle of incidence of the incident radiation. For resonant irradiation the reflectivity is maximized and the intensity forms a standing wave with amplitude that peaks in the vacuum outside the surface and decays with distance into the mirror. (See fig. 6) For most MLMs, the resonance condition strongest only for a limited range of angles (±5º) and a narrow band of wavelengths (~0.6 nm for our MLMs). Because of the dramatic variation in intensity produced by the standing wave under resonant irradiation, the rates of EUV-induced processes responsible for carbonization and/or oxidation could be quite different for resonant and non-resonant irradiation.

Figure 6 shows the intensity standing wave at resonance as a function of position near the surface calculated for the Ru-capped mirrors discussed here. These mirrors were designed so that the minimum intensity, or node, occurs near the Ru-on-Si interface approximately 2 nm from the Ru surface as shown. Of the two processes driving photo-induced surface chemistry, direct photo-excitation and excitation by secondary electrons, it is predominantly the low-energy secondary electrons that cause the oxidation and carbonization that lead to the loss in reflectivity.[9] A more detailed model of the secondary electron yield (SEY) can be found in [Ref.10], but the essential physics is captured by

$$SEY \propto \int I_s(z) e^{-z/\delta} dz \qquad \text{(Eq. 1)}$$

where $I_s(z)$ is the intensity of the standing wave as a function of depth, and $e^{-z/\delta}$ is the probability that electrons with an average escape depth of δ will be ejected. For most materials δ is approximately 1 nm for the ~10 eV electrons that dominate the photoelectron spectrum.[10,11] So the SEY will be determined primarily by the EUV intensity 1-2 nm nanometers below the mirror surface.[12] For the resonant case depicted in Fig. 6, the nodes are more or less fixed in position relative to the many Mo-Si bilayers regardless of the thickness of the capping layer. Klebanoff, *et al* [Ref. 13] directly demonstrated this relationship between SEY and the location of the surface in the standing-wave field by observing an oscillation in the photo-emission current for MLMs fabricated with increasingly thick Si capping layers. In the same work, the rate of carbon growth on a MLM with a fixed Si-cap thickness was found to depend on the location of the surface of the deposited carbon layer within the standing wave. The growth rate increased as the advancing front of the carbon buildup pushed into the high-field region of the standing wave and then slowed as the surface of the deposited layer grew through a node. Several cycles of this oscillation in damage rate were observed as many nanometers of carbon were deposited. While these earlier studies were performed on Si-capped MLMs, the underlying correlation of damage rate with SEY should be true for any capping layer.

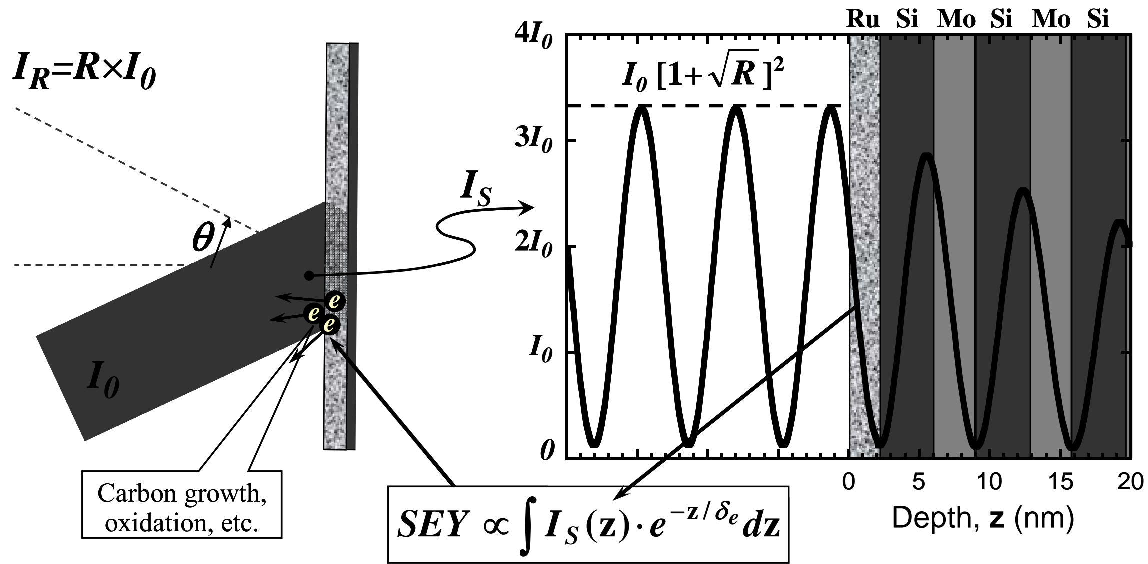

Fig. 6. The intensity interference pattern at the surface of a Ru-capped MLM is plotted in units of the incident intensity,. The amplitude of the intensity standing wave in the vacuum is $I_0(1+\sqrt{R})^2$ which is approximately $3.4I_0$ corresponding to the R = 0.66 of the Ru-capped mirrors discussed here. As demonstrated on Si-capped MLMs the secondary electron yield (SEY) is determined by the field intensity in the first few nanometers below the surface.[13] The reaction rates for oxidation and carbon-growth should depend strongly on the SEY since both processes are driven by low-energy photoelectrons.[9]

Since the wavelength in our lifetime testing chambers is fixed at 13.5 nm, we could not directly observe the response of our MLMs to off-resonance irradiation. Instead we attempted to achieve off-resonance conditions by increasing the angle of incidence from the standard near-design value of 10º to 45º. Figure 7 shows the difference in the calculated intensity for both cases. No standing wave is formed in the 45º off-resonance case, and for the first 2 nm into the multilayer (where the bulk of the photoelectrons are generated) the intensity is only slightly greater than the incident intensity, I_0. For the near-resonant case, however, the intensity of the ensuing standing wave within the mirror varies from slightly greater than $2\times I_0$ at the surface to near zero ~2 nm below the surface. Equation 1 would therefore predict a SEY value nearly equal to I_0 at either angle. So changing the angle of incidence of 13.5 nm radiation should not alter the oxidation and/or carbon-growth rates of our Ru-capped mirrors, which was indeed what was observed in our experiments.

Although the fixed exposure conditions and mirror design prevented a direct demonstration of how on and off-resonance irradiation could affect mirror damage rate, resonance effects could influence the accuracy of lifetime testing under different conditions. Take the case of a mirror designed to have a node of the standing wave at its surface. If its lifetime were tested by illumination with identical intensities, I_0, of broadband and resonant radiation, the intensity at the surface in the broadband case would be I_0, while the intensity under resonant irradiation would be near zero. One might expect that the much lower SEY in the resonant case would lead to a dramatically longer lifetime than that under broadband irradiation. Alternatively, if the illumination in the production environment results in the mirror surface being near the maximum of the standing wave, broadband testing could overestimate the lifetime by nearly a factor of three! This also implies that the damage rate for a given capping layer could vary significantly when deposited on MLMs with different resonant conditions.

In addition to resonance effects of the MLM, the SEY can vary due to the wavelength dependence of the photoionization cross section of the material itself. Yakshinskiy *et al*. [Ref. 12] have shown that the variation of SEY with wavelength is similar for a Ru-capped MLM and the Ru(0001) surface of a Ru crystal. This demonstrates that the wavelength dependence of a Ru-capped MLM is basically determined by the Ru photoionization cross section. In this

same work the SEY was found to vary by nearly a factor of 2 over the wavelength range 10.5 nm to 15.5 nm, which is similar to the bandwidth of exposures performed with Xe-plasma-based pulsed sources with only a Zr spectral filter. Again, this is a potential source of error when predicting optics lifetime based on broadband, non-resonant testing.

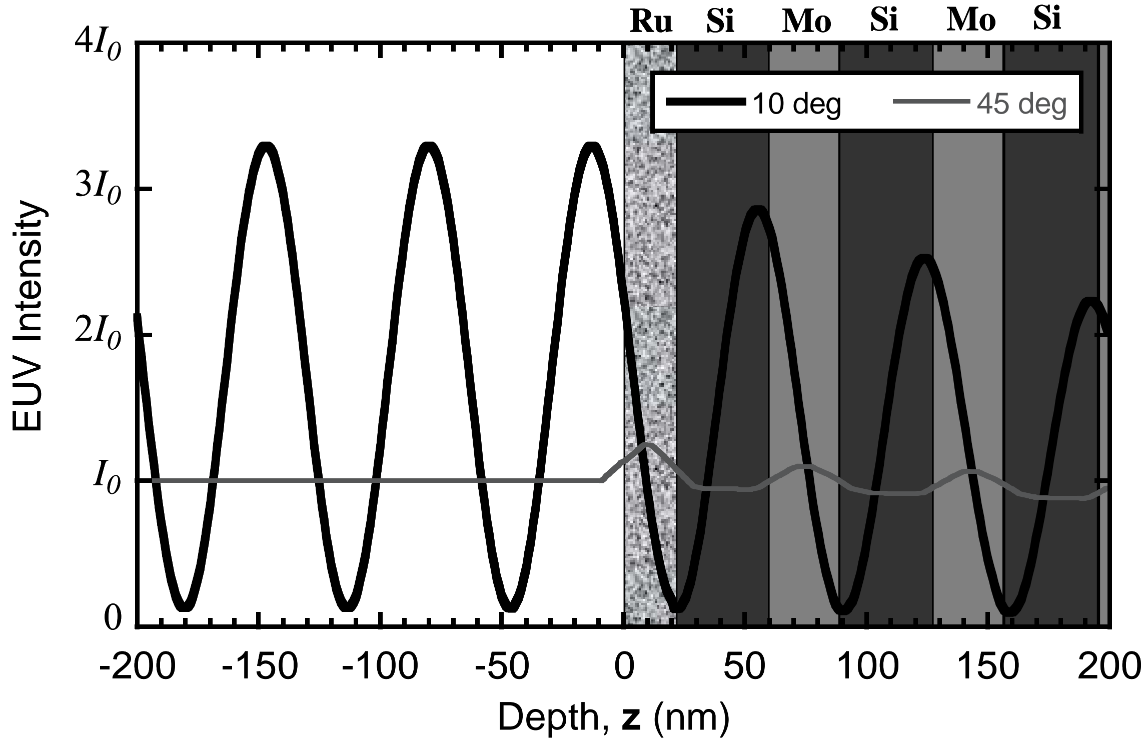

Fig. 7. Calculated intensity values near our Ru-capped MLMs designed for maximum reflectivity of 13.5 nm radiation at a 6º angle of incidence. The distributions shown are for 13.5 nm radiation with incident intensity I_0 and angle of incidence 10º and 45º. For the near-resonance case (10º) the intensity of the radiation forms a strong standing wave in the vacuum which decays with depth into the mirror. Since the reflectivity is much less than 1 for the far-off-resonance case (45º), there is no reflected beam to form an interference pattern. So the intensity near the surface remains equal to I_0.

4. SUMMARY

We report the results of endurance testing of Ru-capped MLMs using the two synchrotron-based facilities for long-term and accelerated lifetime testing at NIST. High-spatial-resolution reflectometry of the damage spot resulting from a single ten-hour exposure of Ru-capped MLM yields information on the reflectivity loss as a function of intensity (or dose) over the Gaussian spatial distribution of the EUV beam. Results from both chambers reveal highly non-intuitive relationships between reflectivity loss and admitted water vapor partial pressure, ambient background gases, hot filaments in the chamber, EUV and doses from. The inverse dependence of reflectivity loss on H_2O pressure over the range $2x10^{-7}$ Torr to $5x10^{-6}$ Torr is most prominent for EUV doses greater than ~100 J/mm^2 in an environment with no hot filaments. When the MLMs are exposed in the vicinity of an ion gauge filament, however, the reflectivity loss is greatest at low pressures and EUV doses below ~100 J/ mm^2. Even for the fixed H_2O pressure of $5x10^{-6}$ Torr, the evolution of reflectivity loss with EUV is not straightforward. We find that there is an initial, rapid ~1.3% decrease in reflectivity during the first ~100 J/ mm^2 followed by a recovery of 0.6% over the next ~300 J/ mm^2 followed by a slow, approximately linear decay with dose. These nonlinearities appear more pronounced at our highest intensity ~8mW/mm^2.

We conjecture that these highly nonlinear behaviors may be the result of competition between oxidation and carbon-deposition processes. Since C and Ru have overlapping XPS spectra, the evolution of surface carbon on Si-capped MLMs exposed in 5×10^{-7} Torr of water vapor was measured by XPS. These results suggested that there could be an initial cleaning of the native surface carbon followed by the deposition of another carbon species induced by EUV+H_2O exposure. The source of this carbon growth is not apparent since the only carbon-containing species present in the RGA mass spectrum are CO and CO_2, and ancillary exposures in admixtures of water and admitted CO or CO_2 produced the same results as exposures in water alone. It is possible that stray EUV radiation (such as the reflected beam) produces reactive carbon-containing species that are neutralized by the first surface they strike, which could be the sample. Such a line-of-sight contamination scenario would not be detectable by a quadrupole mass spectrometer. Experiments are currently underway to test this hypothesis.

The non-intuitive results presented here suggest that predicting MLM lifetime based on accelerated testing is not straightforward and could produce very misleading results determined by environmental conditions that are difficult to monitor and control. This suggests that any lifetime testing procedure involve duplicate exposures to check for consistency, and, if test conditions do not exactly match the production environment, tests should be performed in multiple facilities to reveal unexpected dependencies.

REFERENCES

[1] L. R. Canfield and N. Swanson, “Far ultraviolet detector standards”, *J. Res. NBS* **92**, 97-112 (1987).
[2] C. Tarrio, R. N. Watts, T. B. Lucatorto, M. Haass, T. A. Calcott, and J. Jia, "New NIST/DARPA National Soft X-ray Reflectometry Facility", *J. X-ray Sci. Tech*. **4**, 96 (1994).
[3] C. Tarrio and S. Grantham, “A synchrotron beamline for extreme-ultraviolet multilayer mirror endurance testing”, submitted *to Rev. Sci. Instrum*.
[4] Saša Bajt, Zu Rong Dai, Erik J. Nelson, Mark A. Wall, Jennifer B. Alameda, Nhan Q. Nguyen, Sherry L. Baker, Jeffrey C. Robinson, John S. Taylor, “Oxidation resistance and microstructure of ruthenium-capped extreme ultraviolet lithography multilayers”, *J. Microlith., Microfab., Microsyst.* **5**, 023004 (2006)
[5] S. B. Hill, I. Ermanoski, S. Grantham, C. Tarrio, T. B. Lucatorto, T. E. Madey, S. Bajt, M. Chandhok, P. Yan, O. Wood, S. Wurm and N. V. Edwards, “EUV testing of multilayer mirrors: critical issues”, *Proc SPIE* **6151** (2006)
[6] L.E. Klebanoff, M.A. Malinowski, W.M. Clift, C. Steinhaus, and P. Grunow, “Use of gas-phase ethanol to mitigate extreme UV/water oxidation of extreme UV optics”, *J. Vac. Sci. Technol. A* **22,** 425 (2004).
[7] I. Nishiyama, H. Oizumi, K. Motai, A. Izumi, T. Ueno, H. Akiyama, and A. Namiki, "Reduction of oxide layer on Ru surface by atomic-hydrogen treatment", *J. Vac. Sci. Technol. A* **23**, 3129-3131 (2005)
[8] T. E. Madey, “Summary Abstract: Surface phenomena and their influence on ultrahigh vacuum gauges,” *J. Vac. Sci. Technology* **A5**, 3249 (1987)
[9] T. E. Madey, N. S. Faradzhev, B. V. Yakshinskiy, and N.V. Edwards, "Surface phenomena related to mirror degradation in extreme ultraviolet (EUV) lithography", *Appl. Surf. Sci.* **253**, 1691-1708 (2006)
[10] J. Hollenshead and L. Klebanoff, "Modeling radiation-induced carbon contamination of extreme ultraviolet optics", *J. Vac. Sci. Technol. B* **24**, 64-82 (2006)
[11] S. Tanuma, C.J. Powell, and D.R. Penn, "Calculations of electron inelastic mean free paths for 31 materials", *Surf. Interf. Anal.* **11**, 577-589 (1988)
[12] B. V. Yakshinskiy, R. Wasielewski, E. Loginova, and Theodore E. Madey, “Carbon accumulation and mitigation processes, and secondary electron yields of ruthenium surfaces”, *Proc SPIE* **6517** (2007)
[13] M. Malinowski, C. Steinhaus, M. Clift, L. E. Klebanoff, “Controlling Contamination in Mo/Si Multilayer Mirrors by Si Surface-capping Modifications, *Proc. SPIE* **4688** (2002)